Integration of a Wearable Interface in a Design-to-Robotic-Production and -Operation Development

A. Liu Cheng[a,b], H. H. Bier[a,c], and S. Mostafavi[a,c]

[a]Faculty of Architecture and the Built Environment, Delft University of Technology, Delft, The Netherlands
[b]Facultad de Arquitectura e Ingenierías, Universidad Internacional SEK, Quito, Ecuador
[c]Dessau Institute of Architecture, Anhalt University of Applied Sciences, Dessau, Germany
E-mail: a.liucheng@tudelft.nl, h.h.bier@tudelft.nl, s.mostafavi@tudelft.nl

Abstract –

This paper presents the integration of an *Internet of Things* wearable device as a personal interfacing node in an intelligent built-environment framework, which is informed by *Design-to-Robotic-Production and -Operation* principles developed at *Delft University of Technology*. The device enables the user to act as an active node in the built-environment's underlying *Wireless Sensor and Actuator Network*, thereby permitting a more immediate and intuitive relationship between the user and his/her environment, where this latter is integrated with physical / computational adaptive systems and services. Two main resulting advantages are identified and illustrated. On the one hand, the device's sensors provide personal (i.e., body temperature / humidity, physical activity) as well as immediate environmental (i.e., personal-space air-quality) data to the built-environment's embedded / ambulant systems. Moreover, rotaries on the device enable the user to override automatically established illumination and ventilation settings in order to accommodate user-preferences. On the other hand, the built-environment's systems provide notifications and feedback with respect to their status to the device, thereby raising user-awareness of the state of his/her surroundings and corresponding interior environmental conditions. In this manner, the user becomes a context-aware node in a *Cyber-Physical System*. The present work promotes a considered relationship between the architecture of the built-environment and the *Information and Communication Technologies* embedded and/or deployed therein in order to develop highly effective alternatives to existing *Ambient Intelligence* solutions.

Keywords –

Design-to-Robotic-Production & -Operation, Internet of Things, Ambient Intelligence, Wireless Sensor andNetworks, Adaptive Architecture.

1 Background and Introduction

The present work is situated at the intersection of the *Ambient Intelligence* (AmI) [1] and the *Adaptive Architecture* (AA) [2, 3] discourses. While AmI promotes a vision of future dwelling spaces integrated with sophisticated systems built on *Information and Communication Technologies* (ICTs), AA approaches the same endeavor via both high- and low-tech [4] architectural devices as well as physical transformations in order to instantiate active, reactive, and interactive built-environments. A common denominating objective of both AmI and AA is the promotion and prolongation of occupant well-being via built-environments capable of adapting to user-preferences as well as of encouraging healthy habits via non-invasive feedback loops (e.g., [5, 6]). At present, there are research groups and/or projects developing expressions of similar intelligent built-environments (e.g., [7–9]) via a variety of approaches. In this development, *Design-to-Robotic-Production & -Operation* (D2RP&O) [10] principles developed at *Delft University of Technology* (TUD) are used. D2RP&O extends beyond the AmI and AA discourses to conceive of built-environments imbued with high-resolution intelligence whose architectural and ICTs considerations mutually inform one another from the early stages of the design process. More specifically, D2RP promotes material and formal intelligence via geometry-optimization and heterogeneous material composition as well as *componentiality* and *hybridity* principles [11], while D2RO promotes the integration and deployment of sophisticated robotic as well as computational agents and mechanisms within the D2RP-informed architecture. In this manner, the sophistication of the physical built-environment as well as that of its ICTs mutually correspond to and complement one another, which results in more intuitive and effective solutions.

The present implementation builds on a D2RP&O-enabled system architecture previously developed by the authors [12]. The *Internet of Things* (IoT) wearable device (wearable, henceforth) described develops the

Wearables subsystem of said system architecture in order to render the user a *de facto* context-aware node in its *Wireless Sensor and Actuator Network* (WSAN), which underlies the *Cyber-Physical System* (CPS) that is the built-environment with its physical / computational mechanisms and services. Consequently, the built-environment is able to access user-specific physical / environmental data to consider in conjunction with data gathered by architecture-embedded sensors, which together enable the system's decision-making mechanism to yield highly informed actuations sensitive to the user. Similarly, the user is made aware of the status of his/her built-environment and of its interior environmental conditions, enabling direct or wireless intervention. This expression of intelligence in the built-environment supervenes on human and non-human collaboration.

2 Concept and Approach

The present implementation is divided into two main components developed in parallel, one corresponding to D2RP (see Section 3.1) and another to D2RO (see Section 3.2). Although the development focuses on a wearable belonging to D2RO systems, its proper operation requires the establishment of a WSAN that includes architecture-embedded nodes with which to exchange data and/or to instigate actuations. Such embedded nodes are integrated into architectural components specifically designed via D2RP to accommodate them in a seamless and considered manner. In this configuration, the very architecture of the built-environment is able to complement the technical sophistication of the wearable deployed within it. Without the architecture-embedded ICTs, the operability of the wearable would be limited to the services enabled by its own sensors, which would only provide information about the immediate surroundings of the user, leaving him/her unaware of the interior environmental conditions of the remaining surroundings. Moreover, without complementing architecture-embedded ICTs, the wearable would be unable to engage remotely with mechanism inherent in adaptive architectures.

In the present setup, real-scale architectural fragments composed of robotically fabricated components are developed via material subtraction in D2RP in order meet a variety of environmental, structural, and functional requirements as well as to host said embedded nodes (see Figure 1). That is to say, from the early stages of the design process, the envisioned technological services are taken into consideration along typical architectural considerations. In this manner, the resulting components are deliberately fabricated to sustain adaptive mechanisms in the form of computational services as well as in physical actuations in the built-environment.

With an established complementary infrastructure, four instances of the presented wearable—worn by four different users occupying the same built-environment—are developed and integrated into the WSAN via *Bluetooth Low Energy* (BLE). These wearables exchange sensor data and/or actuation commands with two coordinating nodes as well as with six router nodes, which in turn exchange data and/or actuation commands with one another via ZigBee, BLE, and/or WiFi (depending on distance, frequency, and/or latency requirements). This limited setup is intended to demonstrate seamless interoperability with respect to heterogenous microcontrollers / development platforms as well as to communication protocols within the WSAN.

Each wearable is equipped with eight attached sensors, regulators, and LED-bar displays, viz.: (1) an *MQ-4 Air-Quality* sensor to gauge air-quality within the user's personal space; (2) a *DHT-22 Temperature and Humidity* sensor to ascertain the user's thermal comfort; (3) an illumination override rotary as well as (4) a ventilation override rotary to enable the user to deviate from prescribed standards according to preference; (5) a notification confirmation button to acknowledge sent notifications by other WSAN nodes; (6) a notification buzzer to enable other WSAN nodes to provide audible prompts; (7) a LED-bar indicator of human presence or environmental events (e.g., gas-leaks, etc.) in any of six presently defined regions within the built-environment to notify the user; and (8) a LED-bar indicator of the immediate air-quality to warn the user of personal-space air-contamination levels. Additionally, the *Microcontroller Unit* (MCU) on which the wearable is based is integrated with a *BOSCH BMA250E triaxial accelerometer*, which may be used for gathering spatial displacement data for latter *Human Activity Recognition* (HAR) (see Figure 2 and Section 3.2). The functional advantage of these attached and integrated mechanisms is discussed in Section 3and demonstrated in Section 4.

Finally, the values and states of each mechanism of every wearable-instance are relayed to any of the architecture-embedded nodes for real-time streaming to Plotly© [13] for remote visualization and/or subsequent analysis of gathered datasets (within cloud-service storage limits) (see Figure 3).

3 Methodology and Implementation

3.1 Design-to-Robotic-Production: Intelligent Architectural Components

The developed D2RP components are considered from three different perspectives, each pertaining to a different set of functional requirements and scale—i.e., *Macro*, *Meso*, and *Micro*—in order to yield geometries with deliberate densities and porosities (see Figure 1).

Figure 1. Robotically fabricated components via material subtraction in D2RP. Left-to-Right: Single-layer physical prototype, (1) front-view and (2) side-view; Virtual 3D model, (3) single-layer side-view and (4) double-layer (inner and outer) side-view. Concept by Chong Du, Jihong Duan, and Floris van Buren [14].

The components are fabricated from Styrofoam blocks via material subtraction with a 6-axis KUKA robot [15]. From the *Macro* perspective, human movement is mapped unto an initial geometry with data from human body-posture analysis. The resulting form is optimized via structural analysis, consideration of environmental conditions and loads (e.g., wind direction and loads, etc.), and solar radiation with respect to a specified geographical location. Throughout this process, *componential* principles inform the design, which ensures that differentiated components are deliberately fabricated to conform seamlessly with one another to yield a unified whole. Furthermore, *hybridity* principles enable material heterogeneity within specific components as required by functional considerations. For example, structural analysis identifies areas across the geometry that are subjected to tension, compression, shear, bending, and torsion forces. The components within which these areas are located require deliberate material heterogeneity in order to properly account for said forces while preserving componential principles

From the *Meso* perspective, each component is designed to consist of two irregular yet mutually complementary layers—one external and one internal (see Figure 1, item 4)—while conforming a middle cavity as a continuous air-channel. Moreover, other cavities across both layers are designed to integrate mechanized cooling, heating, ventilation, and illumination systems, where their operation is controlled by architecture-embedded nodes in the built-environment's WSAN.

From the *Micro* perspective, variation of densities and porosities at the material level are considered with respect to functional requirements related to natural illumination and ventilation as well as to the potential for particular views.

3.2 Design-to-Robotic-Operation: Bluetooth Low Energy Wearable node

The developed D2RO wearable is built with a battery-powered PunchThrough© LightBlue Bean+™ (LBB+) MCU, a corresponding *Groove Expander*, and the eight previously listed mechanisms (see Figure 2, *WSAN/BAN: BLE Wearable Node*). The four instances of this wearable exchange data (via BLE) with two Raspberry Pi© 3 Model B™ (RPi3) *Single-Board Computer* (SBC) coordinating nodes as well as with six router nodes—i.e., three Asus© TinkerBoard™ SBCs and three Intel© Joule™ system on modules (see Figure 2, *WSAN: Arch. Embedded Nodes*)—which exchange data via ZigBee, BLE, and WiFi. These six nodes correspond to the six defined regions in the built-environment of this setup. As mentioned earlier, this heterogeneity in systems and communication protocols serves to highlight the effective interoperability between diverse ICTs within the WSAN. Nevertheless, these specific ICTs are deliberately included in the WSAN for their individual capabilities.

For example, all of the presently mentioned coordinating and router nodes may be dynamically clustered together *ad hoc* for Machine Learning activities as described and implemented by the authors elsewhere [12].

In the inherited and presupposed system architecture, a variety of environmental sensors monitor the *Interior Environmental Quality* (IEQ) [16] of the inhabited space. Whenever sensed-data deviates from prescribed illumination, ventilation, cooling, and heating standards, mechanical systems are activated in order to restore and sustain values within optimal thresholds. The wearable adds another dimension of sensing and aids the built-environment's decision-making mechanisms in accurately gauging the environmental conditions of the inhabited space, while simultaneously raising awareness in the user via its notification / feedback mechanisms.

In order to describe how this wearable does this, the implementation and functionality of each one of its attached and embedded mechanisms is described as follows:

1. *MQ-4 Air-Quality sensor*: This sensor has a methane-gas detection range of 300-10,000 *parts-per million* (ppm) [17]. Its purpose on the wearable is to detect the immediate air-quality surrounding the user. Should the built-environment's embedded-sensors fail to perceive contamination, the wearable's air-quality sensor instigates localized ventilation mechanisms nearest to the user to activate. In order to reduce unnecessary energy-consumption, the sensor is programed to take a reading every ten minutes. However, if sudden deterioration of air-quality is detected, the frequency increases to five minutes.

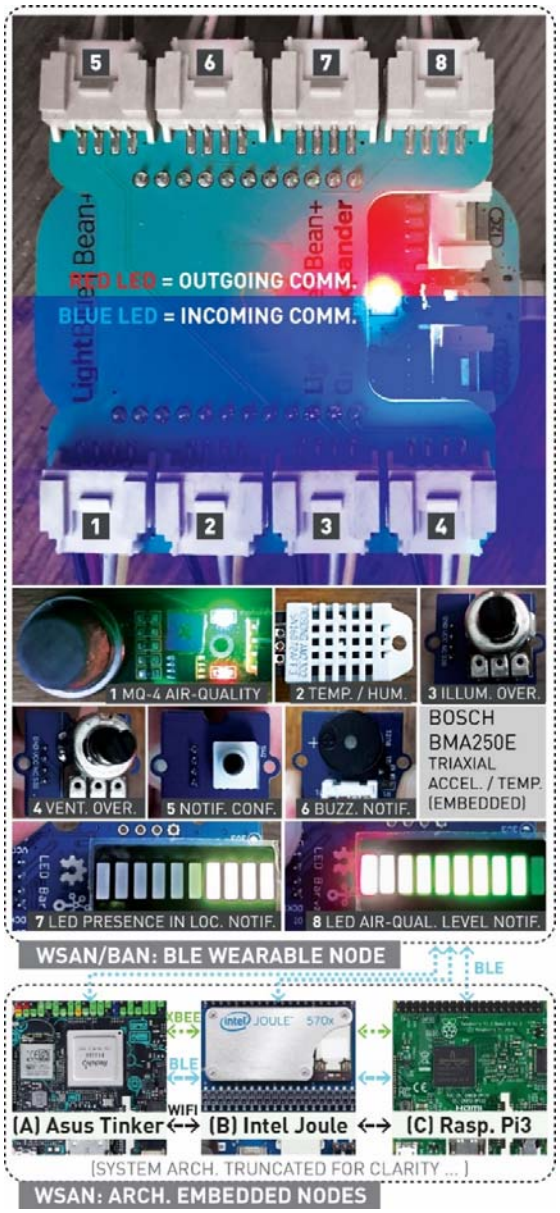

Figure 2. BLE Wearable Node as WSAN / BAN, Features.

2. *DHT-22 Temperature and Humidity sensor*: This sensor detects the temperature and humidity within the user's personal space. Like the previous sensor, if it detects deviations from optimal thresholds (in conjunction with or independently of architecture-embedded counterparts), localized cooling or heating mechanisms activate to sustain user comfort. Since the probabilities of a sudden drop in temperature and humidity within an enclosed environment are low, the sensor is configured to take readings every half hour.
3. *Rotary Illumination override*: This rotary mechanism enables the user to override illumination settings automatically determined by the built-environment's decision-making mechanism, should personal preferences deviate from optimal standards. Unlike the previous two sensors, this mechanism does not have a predetermined activation interval, as its activation requires the user's manual rotation.
4. *Rotary Ventilation override*: This rotary mechanism performs as the previous one only with respect to ventilation. The IEQ-sustaining mechanisms in the built-environment are configured to maintain conditions within *Comité Europeen de Normalisation* (CEN) Standard EN15251-2007 [18] thresholds, but precedence is assigned to human prerogative. Contingency measures limiting this override prevent sustained over-heating or over-cooling detrimental to human well-being.
5. *Notification Acknowledgement button*: There may be instances when the built-environment attempts to notify the user of urgent environmental events and/or conditions in particular regions (see item 7). This button serves to acknowledge such notifications.
6. *Notification Buzzer*: Two kinds of notification are implemented for this paper, one using visual cues (see items 7 and 8) and the other using sound. This buzzer is used only for urgent notifications, where a range of tones correspond to varying degrees of urgency. This mechanism works in conjunction with items 7 and 5.
7. *LED-bar "Presence / Event in Location" notification*: This LED-bar represents a visual cue that notifies the user of either human presence in a given regions of the built-environment or environmental events and/or conditions in those regions. For example, with respect to its *notification of human presence* function, the user may be notified of the presence of other users in any of the six hypothetical regions defined in this setup. It may be observed in Figure 2 that this LED-bar indicates that four regions are occupied by other users. With respect to its *notification of environmental events and/or conditions* function, it may be that a given region has detected a gas-leak, and in this case the LED corresponding to that region would turn red and the buzzer (i.e., item 6) would require acknowledgement via the notification button (i.e., item 5). The architecture-embedded ventilation mechanisms themselves would automatically intervene in such a scenario, but the user is notified to raise awareness of his/her surroundings.

8. *LED-bar "Air-Quality in personal space" notification*: This LED-bar works in conjunction with item 1 and serves to inform the user of the air-quality of his immediate surroundings. In order to prevent unnecessary energy-consumption, this visual cue only activates when the user raises his/her arm in a specific gesture—a mechanism adapted from Fitbit© Activity Trackers such as the *Charge HR*™, which also belongs to the *Wearable* subsystem of the inherited WSAN.

Finally, the embedded *BOSCH triaxial accelerometer* is used for HAR as a secondary data-source, if a primary accelerometer-enabled smart-device is absent from the ecosystem. This is due to the energy-consumption of continuous streaming of accelerometer data. In the inherited system architecture, HAR via smartphones [19] is preferred.

4 Results and Discussion

As mentioned in earlier sections, in the present setup four instances of the wearable are developed and used in a built-environment containing six defined regions, each one monitored via real-time streaming of the data generated / gathered by its attached and embedded mechanisms to Plotly in different frequencies—for example, accelerometer data frequency, for purposes of HAR, must be higher than that of the Temperature and Humidity sensor. Since the wearables only work with BLE, their generated / gathered data is streamed to any of the architecture-embedded nodes, where each may write directly to data streams pertaining to the attached and embedded mechanisms of any of the wearables. All the data emitted by the wearables include a device identifier which is used to ascertain that each of their corresponding data is fed to the correct Plotly stream. In this section, the Plotly charts corresponding only to one wearable— shown in Figure 3—are discussed (from top to bottom).

The first chart in Figure 3 shows that in that particular instance of the test-run, the air-quality surrounding the user is consistent, which is expected from a built-environment integrated with self-regulating ventilation devices. The values of the *y-axis* range from 1 to 0, where 1 attains optimal standards.

In the test-run interval corresponding to the *temperature* component of the second chart (i.e., chart 2a), the user first manually overrides automatic settings to increase ventilation, resulting in a deviation from the optimal temperature of 22.5° C.—an average of the accepted human-comfort range of 21° C. – 24° C. [20]. That is, it may be observed that between the 7,180th and 7,190th reading the actual sensed temperature dropped to ~55% of 22.5° C.

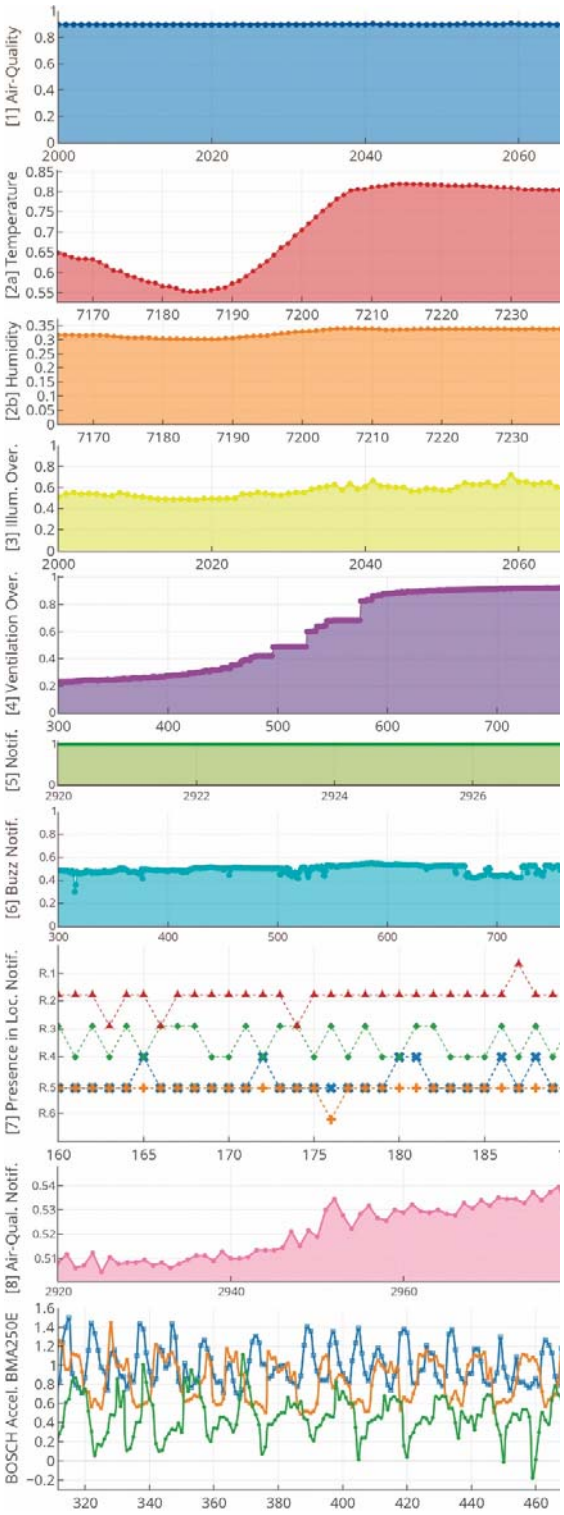

Figure 3. Gathered data plotted in real-time in Plotly©.

After this interval, and with no further human override, the temperature climbed steadily to more comfortable temperatures. The *humidity* component of this chart (i.e., chart 2b) indicates a slight decrease in humidity when ventilation systems were manually engaged, which is an expected result of higher air-flow.

The third chart indicates how much of the automatically determined values of illumination intensity is actually permitted to shine. That is to say, the illumination overriding mechanism works as a function of the built-environment determined output. For example, it may be observed in this chart that throughout this test-run interval, the actual illumination was kept between only ~50% to almost ~80% of the prescribed intensity-levels.

In the fourth chart, automatically determined temperature levels were decreased to ~21% of the actual values and gradually increased to ~90%.

The fifth and simplest chart records no instance of notification acknowledgements. The visualization of *pressed* vs. *unpressed* is inverted, where instances of the former are shown as 0 and of the latter as 1. Accordingly, no instance of notification acknowledgement is registered throughout the test-run, which corresponds to no undesirable environmental events being detected in any of the regions of the built-environment.

Urgent notifications result from a function over environmental readings. For example, it is not the case that any air-contamination triggers an urgent prompt, as healthy environments invariably contain degrees of air-contaminants, only within negligible levels. Accordingly, an urgent phenomenon is gauged based on the concentration and duration of undesired contaminants—in the present case, of methane gas, which has a *Threshold Limit Value* (TLV) of 1,000 ppm during an 8-hour period [21]. It is observed from the fifth chart that no notification acknowledgement instances are registered in the test-run's interval, which suggests an absence of urgent environmental events. This, however, does not suggest that the environmental conditions of any of the six regions are optimal. At most, it suggests that no air-contamination levels exceed accepted limits. This may be observed in the sixth chart—corresponding to the *buzzer* notification—where methane levels are detected at ~50% of a the prescribed TLV. Note that there are no instances below ~30%, since the sensor's lower-bound limit is 300 ppm.

The seventh chart maps the presence of the four users (each with a wearable, represented in red, green, blue, and orange) with respect to the six predetermined regions in the built-environment. The present set of charts correspond to the user in red. Unlike the other charts, this one in particular is common to all wearable users, which enables everyone in within the same built-environment to know one another's location.

The eighth chart, which corresponds to the LED-bar Air-Quality notification or indicator, indicates up to which LED is turned on in accordance with the air-quality ascertained (see the first chart). The *y-axis* ranges from 0 – 1, where 0 corresponds to no LEDs being turn on, 0.5 to five being on, and 1 to all being on. In this chart, it is observed that ~5 LEDs in the LED-bar were on during the corresponding test-run interval. As with the sixth chart and corresponding mechanism, the LED-bar corresponding to air-quality is driven by a function over air-quality readings, which explains the high-precision of logged values in this chart. Although at first glance it may appear simpler to define eleven possible states (i.e., 0-10) to correspond to the air-quality range of zero to ten, where high precision air-quality values with several decimals are simply rounded to the nearest single digit decimal. But this is redundant, as the eighth chart demonstrates that the present mechanism is capable of turning five LED bars on whenever the value ranges anywhere within 0.5, regardless of trailing decimal places.

Finally, the last chart—corresponding to the MCU-embedded triaxial accelerometer—demonstrates that three-dimensional displacement data is accurately logged and plotted by the present setup. As mentioned at the end of Section 3, it is preferred that accelerometer data-gathering be relegated to another smart-device (e.g., smartphone) due to the energy-consumption involved in high-frequency data transmission. However, if no such alternative is present, the wearable's accelerometer fulfills this task.

5 Conclusions

The present paper detailed the development of a wearable device to complement and to be complemented by ICTs embedded in intelligent and robotically fabricated architectural components via material subtraction in D2RP. In conjunction, said wearable and architecture-embedded systems provide higher precision and fidelity in the continuous promotion of user well-being in the built-environment, which the authors argue is a necessary feature for effective alternatives to existing AmI solutions. In the limited setup and corresponding test-run, the wearable performed as expected of a prototype, although aspects for latter optimization were indeed identified. A more efficient approach to energy consumption is to be developed in order to render the device a viable system in built-environments subsuming *high-resolution intelligence*.

Moreover, the majority of attached mechanisms will be embedded in the device in subsequent developments, which would require a custom-designed MCU. This will reduce the size of the wearable as well as moderately increase its battery-life.

Furthermore, the LED-bar indicating the position of users across regions in the built-environment will be reconsidered, as the present hardware limits the number of regions monitored to ten (i.e., ten LED bars in the module). Present work is being undertaken to replace the LED-bars with a low-energy *electrophoretic display*—i.e., Plastic Logic©'s 1.1" Lectum® display [22].

Finally, ZigBee communication capabilities are also presently being added unto the device in order to extend its longer-range data exchange capabilities.

Acknowledgement

This paper has profited from the contribution of TUD Robotic Building researchers, tutors, and students. In particular, the authors acknowledge students Chong Du, Jihong Duan, and Floris van Buren for the conceptual development of a student housing unit as well as its corresponding real-scale fragment.

References

[1] E. Zelkha, B. Epstein, S. Birrell, and C. Dodsworth, "From Devices to 'Ambient Intelligence': The Transformation of Consumer Electronics (Conference Keynote)," in *Digital Living Room Conference*, 1998.

[2] H. Schnädelbach, "Adaptive architecture," *interactions*, vol. 23, no. 2, pp. 62–65, 2016.

[3] K. E. Green, *Architectural robotics: Ecosystems of bits, bytes, and biology*. Cambridge, Massachusetts: The MIT Press, 2016.

[4] B. Kolarevic, "Outlook: Adaptive Architecture: Low-Tech, High-Tech, or Both?," in *Applied Virtuality Book Series*, v.8, *ALIVE: Advancements in adaptive architecture*, M. Kretzer and L. Hovestadt, Eds, Basel/Berlin/Boston: Birkhäuser, 2014, pp. 148–157.

[5] G. Acampora, D. J. Cook, P. Rashidi, and A. V. Vasilakos, "A Survey on Ambient Intelligence in Healthcare," *Proc. IEEE*, vol. 101, no. 12, pp. 2470–2494, 2013.

[6] A. Liu Cheng and H. H. Bier, "An Extended Ambient Intelligence Implementation for Enhanced Human-Space Interaction," in *Proceedings of the 33rd International Symposium on Automation and Robotics in Construction (ISARC 2016)*, 2016, pp. 778–786.

[7] J. A. Kientz, S. N. Patel, B. Jones, E. Price, E. D. Mynatt, and G. D. Abowd, "The Georgia Tech aware home," in *CHI '08: The 26th annual CHI Conference on Human Factors in Computing Systems: April 5-10, 2008 in Florence, Italy*, New York: ACM, 2008, p. 3675.

[8] P. Rashidi and D. J. Cook, "Keeping the Resident in the Loop: Adapting the Smart Home to the User," *IEEE Trans. Syst, Man, Cybern. A*, vol. 39, no. 5, pp. 949–959, 2009.

[9] A. A. Helal, M. Mokhtari, and B. Abdulrazak, *The engineering handbook of smart technology for aging, disability, and independence*. Hoboken, N.J.: Wiley, 2008.

[10] H. H. Bier, "Robotic Building as Integration of Design-to-Robotic-Production & Operation," *Next Generation Building*, no. 3, 2016.

[11] H. H. Bier and S. Mostafavi, "Robotic Building as Physically Built Robotic Environments and Robotically Supported Building Processes," in *Human-computer interaction series, Architecture and interaction: Human computer interaction in space and place*, N. S. Dalton, H. Schnädelbach, M. Wiberg, and T. Varoudis, Eds, Switzerland: Springer International Publishing, 2016, pp. 253–271.

[12] A. Liu Cheng, H. H. Bier, G. Latorre, B. Kemper, and D. Fischer, "A High-Resolution Intelligence Implementation based on Design-to-Robotic-Production and -Operation strategies," in *Proceedings of the 34th International Symposium on Automation and Robotics in Construction (ISARC 2017)*, 2017.

[13] Plotly®, *API Settings.* Available: https://plot.ly/settings/api (2015, Feb. 15).

[14] C. Du, J. Duan, and F. van Buren, *MSc2, Group 2, Student Housing Unit.* Available: http://ip.hyperbody.nl/index.php/Msc2G2:Page4 (2017, Jul. 01).

[15] ____, *Interactive Prototyping, MSc 2 Spring Semester 2017: GROUP 2: Components Production.* Available: http://ip.hyperbody.nl/index.php/Msc2G2:Page4 (2017, Jul. 10).

[16] P. M. Bluyssen, *The healthy indoor environment: How to assess occupants' wellbeing in buildings*. London, New York: Routledge/Taylor & Francis Group, 2014.

[17] Zhengzhou Winsen Electronics Technology Co, Ltd, *Flammable Gas Sensor (Model: MQ-4): Manual version: 1.3, 2014-05-01*. Available: https://cdn.sparkfun.com/datasheets/Sensors/Biometric/MQ-4%20Ver1.3%20-%20Manual.pdf (2017, Jun. 05).

[18] Comité Européen de Normalisation© (CEN), *Standard EN 15251–2007: Indoor environmental input parameters for design and assessment of energy performance of buildings addressing indoor air quality, thermal environment, lighting and acoustics.* Available: http://www.sysecol2.ethz.ch/OptiControl/Literatur

eOC/CEN_06_prEN_15251_FinalDraft.pdf (16/07/07).

[19] J. L. R. Ortiz, *Smartphone-based human activity recognition*. Cham: Springer, 2015.

[20] A. Hartley, "Fuel poverty," *West Midlands Public Health Observatory. Birmingham, UK: West Midlands Public Health Observatory (1 March 2006)*, p. 3, 2006.

[21] The National Institute for Occupational Safety and Health (NIOSH), *International Chemical Safety Cards (ICSC): Methane.* Available: https://www.cdc.gov/niosh/ipcsneng/neng0291.html (2017, Jul. 10).

[22] Plastic Logic©, *Display Platform with Ultrachip UC8156.* Available: http://www.plasticlogic.com/products/displays-with-ultrachip/ (2017, Jun. 07).